Article

Isothermal Titration Calorimetry enables rapid characterisation of enzyme kinetics and inhibition for the human soluble Epoxide Hydrolase

Giancarlo Abis, Raul Pacheco-Gomez, Tam T. Bui, and Maria Rosaria Conte

Isothermal Titration Calorimetry enables rapid characterisation of enzyme kinetics and inhibition for the human soluble Epoxide Hydrolase

Giancarlo Abis[†,‡], Raúl Pacheco-Gómez[§], Tam T.T. Bui[†,¶],

Maria R Conte[†,¶,*]

[†]Randall Centre for Cell and Molecular Biophysics, School of Basic and Medical Biosciences, King's College London, London, SE1 1UL, UK.

[§]Malvern Panalytical Ltd, Enigma Business Park, Grovewood Road, Malvern, WR14 1XZ, UK.

[¶]Centre for Biomolecular Spectroscopy, King's College London, London, SE1 1UL, UK.

*corresponding author: sasi.conte@kcl.ac.uk

[‡]Present address: Division of Bioscience, Institute of Structural and Molecular Biology, University College London, London, WC1E 6BT, UK

1

1
2
3
4
5
6
7
8
9
10
11
12
13
14
15
16
17
18
19
20
21
22
23
24
25
26
27
28
29
30
31
32
33
34
35
36
37
38
39
40
41
42
43
44
45
46
47
48
49
50
51
52
53
54
55
56
57
58
59
60

Abstract

Isothermal titration calorimetry (ITC) is conventionally used to acquire thermodynamic data for biological interactions. In recent years, ITC has emerged as a powerful tool to characterise enzyme kinetics. In this study, we have adapted a single-injection method (SIM) to study the kinetics of human soluble epoxide hydrolase (hsEH), an enzyme involved in cardiovascular homeostasis, hypertension, nociception and insulin sensitivity through the metabolism of epoxy-fatty acids (EpFAs). In the SIM method, the rate of reaction is determined by monitoring the thermal power while the substrate is being depleted, overcoming the need for synthetic substrates, and reducing postreaction processing. Our results show that ITC enables the detailed, rapid and reproducible characterisation of the hsEH-mediated hydrolysis of several natural EpFA substrates. Furthermore, we have applied a variant of the single-injection ITC method for the detailed description of enzyme inhibition, proving the power of this approach in the rapid screening and discovery of new hsEH inhibitors using the enzyme's physiological substrates. The methods described herein will enable further studies on EpFAs metabolism and biology, as well as drug discovery investigations to identify and characterise hsEH inhibitors. This also promises to provide a general approach for the characterisation of lipid catalysis, given the challenges that lipid metabolism studies pose to traditional spectroscopic techniques.

Introduction

Human soluble Epoxide Hydrolase (hsEH – EC 3.3.2.10) is a bifunctional enzyme composed of two structurally and functionally independent domains.[1,2] The C-terminal domain (CTD) is responsible for the hydrolysis of numerous epoxy-fatty acids (EpFAs), bioactive epoxidation products of mono- and polyunsaturated fatty acids with essential roles in cellular and organism homeostasis.[2–4] hsEH CTD hydrolyses EpFAs *via* a S_N2 nucleophilic attack by D335 on the more accessible carbon of the epoxide ring, forming an alkyl-enzyme intermediate, which is then released by the assisted action of D496 and H524.[1,2,5] The catalytic triad is located in the vertex of a large 'L-shaped' active site, and is surrounded by two hydrophobic surfaces dubbed the W334 niche and the F265 pocket, wherein the aliphatic chains of the EpFAs are accommodated.[1,2,4–6]

The best characterised EpFAs substrates of hsEH CTD are the epoxyeicosatrienoic acids (EETs), epoxy-derivatives of arachidonic acid (ARA)[7] (Figure S1A). Although four EET regioisomers, namely 5(6)EET, 8(9)EET, 11(12)EET and 14(15)EET, have been isolated in several organs,[8] the latter two have been shown to be the predominant ARA epoxidation metabolites.[9] EETs function primarily as endothelial-derived hyperpolarising factors in the cardiovascular system and kidney.[7] They play a role in vasorelaxation and vascular homeostasis, exerting anti-inflammatory and pro-angiogenic actions.[7] The bioavailability of EETs is reduced by hsEH-mediated hydrolysis of their epoxy ring to generate the corresponding vicinal diols, namely dihydroxyeicosatrienoic acids (DHETs) (Figure S1A), which possess a considerably reduced biological activity.[7]

In addition to EETs, hsEH hydrolyses several bioactive epoxy-derivatives of linoleic acid (LA) and α-linoleic acid (ALA), including α- and γ-epoxyoctadecadienoic acids (α/γ-EpODEs), epoxyeicosatetraenoic acids (EpETEs), epoxydocosapentaenoic acids (EpDPEs), and epoxyoctadecaenoic acids (EpOMEs)[10,11] (Figure S1B). The physiological role of α- and γ-EpODEs is yet unknown, although their hydrolysis products, the γ-dihydroxy-octadecadienoic acids (γ-DiHODE), exhibit a moderate positive inotropic effect.[12] EpETEs and EpDPEs show a similar breadth of activities to EETs.[13] Vasodilation, antithrombotic, anti-angiogenic and anti-inflammatory effects have been ascribed to both EpETEs and EpDPEs, as well as diminished tumour growth and metastasis in murine models.[10,14,15] Interestingly, the hsEH-mediated hydrolysis product of 19(20)EpDPE, namely the 19(20)-dihydroxy-docosapentaenoic acid (19(20)DiHDPE), accumulates in the retinas and vitreous humour of diabetic retinopathy patients, as a result of increased expression levels of the

enzyme, and aggravates disease severity by altering the localisation of cholesterol-binding proteins in the cell membrane, and leading to breakdown of endothelial barrier function.[16] Contrary to the largely beneficial physiological effects ascribed to other EpFAs, 9(10)- and 12(13)EpOMEs inhibit mitochondrial respiration in various tissues, leading to cardiotoxicity, renal failure, and adult respiratory distress syndrome,[17,18] albeit cytotoxicity is significantly increased in their sEH-catalysed products, the dihydroxy-octadecaenoic acids (DiHOMEs).[17] Interestingly, a Liquid Chromatography tandem Mass Spectrometry (LC-MS/MS) study revealed that hsEH displays different hydrolytic efficiency towards its various EpFA substrates.[10] Although this work provided a first assessment of catalytic profiles for several epoxy fatty acids, potential drawbacks of this methodological approach include the following: (i) it is a discontinuous method, with potentially non-negligible experimental errors; (ii) it requires several sample manipulation steps that could lead to reproducibility issues; (iii) it is time consuming, technically challenging and expensive. Herein we present an Isothermal Titration Calorimetry (ITC)-based method for the systematic characterisation of hsEH catalytic efficiency towards its EpFAs substrates. By measuring the intrinsic heat of hsEH-mediated hydrolysis of the epoxy-fatty acids in a continuous manner,[19–23] our method circumvents the limiting issue of the lack of physicochemical properties of EpFAs substrates/products that can be monitored in real time in a continuous manner. [19–23] This new ITC application shows promise in the complete and highly reproducible characterisation of hsEH-mediated catalysis of epoxy-fatty acids, with relatively low sample amounts, low costs and rapid acquisition times.

The second goal of our study was to establish an easy and versatile method to measure inhibition properties of sEH antagonists against natural substrates. Given that dihydroxy-fatty acids generated by hsEH exhibit either cytotoxic effects or reduced biological activity compared to their epoxy precursors, pharmacological inhibition of hsEH has emerged as an extremely appealing therapeutic strategy to increase EpFAs bioavailability and reap their beneficial properties.[24–26] Currently screening of hsEH inhibitors is mostly performed *via* a high-throughput spectrofluorimetric assay,[27,28] a fast, economical and highly convenient method, that nonetheless carries the main drawback of not employing physiological substrates. To address this, we have adapted an ITC method developed by Di Trani *et al.*[21] Using a well-known hsEH antagonist as a model system we demonstrate here that this technique holds promise for the quantitative screening of new hsEH inhibitors using endogenous EpFAs substrates.

Experimental Section

Enzyme, substrate and inhibitor sample preparation

Recombinant hsEH CTD was obtained as described.[29] This was shown to be necessary and sufficient for EpFA catalysis, and to retain the same kinetic profile as full length protein.[29] Protein, EpFAs substrates and inhibitor AUDA (12-[[(tricyclo[3.3.1.13,7]dec-1-ylamino)carbonyl]amino]-dodecanoic acid) were prepared as reported in the Supporting information.

Single-injection ITC kinetics measurements

The theoretical basis of kinetic measurements by ITC has been described[19,22,30,31] and details are given in the Supporting information. Briefly, in a single injection ITC experiment the total heat measured is proportional to the apparent enthalpy (ΔH_{app}), and the number of moles of product generated. The reaction rate can be related to the amount of heat generated over time. From the derived Michaelis–Menten plots the affinity for the substrate (K_M), turnover rate (k_{cat}), and catalytic efficiency ($k_{cat}/K_M = K_{sp}$) values can be obtained.

Experiments were performed on MicroCal PEAQ-ITC and MicroCal iTC200 calorimeters (Malvern). An hsEH CTD solution at 250 nM was placed in the sample cell, and a 0.5-1.5 mM substrate solution was loaded in the injection syringe. One single 38 μL injection was performed with a speed of 0.58-0.76 μL sec^{-1}. Controls were carried out as described in the Supporting information. Apparent enthalpy of the reaction, heat rate (dQ/dt) and Michaelis–Menten plots were generated using MicroCal PEAQ-ITC Analysis Software (Malvern).

Progressive inhibition ITC enzyme kinetics measurements

A solution containing 0.5 mM of 14(15)EET and 67.37 nM of AUDA was injected into the cell containing 250 nM of hsEH CTD. Four 9.5 μL injections of 12.5 seconds each were performed at a speed of 0.76 μL sec^{-1}. Control experiments are described in the Supporting information. Apparent reaction enthalpy, dQ/dt rates and Michaelis–Menten parameters were generated using the MicroCal PEAQ-ITC Analysis Software (Malvern). Apparent K_M values (K_M') were obtained[32] and data fitting in GraphPad provided K_M'/K_i ratio[20,21], where K_i is the inhibition constant.

Inhibitory constant measurements with a spectrofluorometric method

AUDA inhibitory potency was tested with a spectrofluorometric method,[28] detailed in the Supporting information.

5

Results

A single-injection ITC method characterises the kinetics of hsEH CTD-mediated hydrolysis of 14(15)EET

To probe the kinetics of EpFA hydrolysis catalysed by hsEH CTD, we employed an ITC single-injection method (SIM).[22,23] The substrate solution in the syringe of the calorimeter was injected in a single step into the sample cell containing the enzyme solution, producing a heat response which endured for as long as the reaction proceeds, returning to baseline when the reaction reached completion and all the substrate had been transformed into product. Rapid catalyses give rise to narrow peaks, whilst slow catalyses generate broad peaks. Whereas the total area of the peak depends on the amount of substrate injected and the apparent enthalpy of the reaction, its shape is governed by enzyme concentration, Michaelis–Menten parameters, rate of substrate injection and intrinsic calorimeter response.[19,21]

14(15)EET, the *par excellence* EpFA substrate of hsEH,[8] was used as a test compound to demonstrate method-applicability and to set up the experimental conditions for this study. Optimisation included varying concentrations of substrate and enzyme, as well as reference power, injection speed and spacing. The curve obtained by injecting 14(15)EET into a solution of hsEH CTD was negative, narrow and deep, indicating a fast reaction (Figure 1A). The ΔH_{app} was calculated by integrating the area under the peak, and the Michaelis–Menten kinetics curve fitting was obtained by manually selecting the window between the end of the injection (maximum substrate concentration, corresponding to saturating enzyme conditions) and the end of the decaying portion of the injection (minimum substrate concentration, corresponding to the beginning of the kinetics curve) (Figure 1B). The software fitting calculates $\{[S]_i; v_i\}$ data points through eq 2 and 3 (Supporting information), building a Michaelis–Menten curve (Figure 1C), thereby providing k_{cat} and K_M values. The catalytic efficiency (K_{sp}) was manually calculated as the k_{cat}/K_M ratio. In the optimal conditions, these experiments gave a k_{cat} of 6.64 ± 1.54 sec^{-1} and a K_M of 12.88 ± 1.94 μM for the hsEH-mediated hydrolysis of 14(15)EET (Table 1). To assess any product inhibition effect, the ΔH_{app} of two subsequent injections was compared: no significant variation was observed (Figure S2A and S2B), demonstrating an absence of product inhibition for this hsEH CTD-mediated hydrolysis reaction.

Kinetic characterisation of hsEH CTD-mediated hydrolysis of all EETs

The experimental method and conditions optimised for 14(15)EET were applied to analyse the hsEH CTD-catalysed hydrolysis of the other regioisomeric EETs. Thermal profiles and Michaelis–Menten parameters significantly differed (Table 1). The hydrolysis of 5(6)EET generated a very small and broad peak (Figure 2A), indicating a low ΔH_{app}. Although it was possible to extrapolate a k_{cat} value of 0.35 ± 0.05 sec^{-1} and a K_M of 46.61 ± 10.98 μM, the error associated with this measurement was considerably greater than for the other EETs, due to the reduced magnitude of the heat response and the inability to reach enzyme saturation[23]. Attempts to perform the experiments with higher substrate concentration in fact resulted in precipitation of the mixture. The experiment with 8(9)EET and 11(12)EET gave a k_{cat} of 1.28 ± 0.19 sec^{-1} and a K_M of 23.10 ± 2.39 μM for the former and a k_{cat} of 4.31 ± 0.16 sec^{-1} and a K_M of 1.74 ± 0.20 μM for the latter. Control experiments to check for substrate autohydrolysis and product inhibition are reported in Figures S2B and S3.

Kinetic characterisation of hsEH CTD-mediated hydrolysis of n-3 and n-6 EpFAs

Beyond the EETs, the enzymatic activity of hsEH towards other EpFAs was measured by ITC. We selected two EpETEs, one EpDPE and one EpOME to cover the chemical scaffold diversity of hsEH substrates. Though belonging to the same chemical class, 8(9)EpETE and 17(18)EpETE exhibited different enthalpy and kinetic values (Figure 3A and B, Table 1). The turnover rate for the 8(9)EpETE was 1.61 ± 0.01 sec^{-1}, significantly higher than for the 17(18)-regioisomer (0.64 ± 0.06 sec^{-1}), and its K_M (9.74 ± 0.13 μM) was almost three times lower than 17(18)EpETE (26.37 ± 4.05 μM). A broad negative peak in the thermal profile was also obtained for 19(20)EpDPE, indicating a slow hsEH CTD-mediated hydrolysis (Figure 3C) described by a turnover rate of 1.62 ± 0.08 μM and a K_M of 26.60 ± 1.21 μM (Table 1). The hydrolysis of 12(13)EpOME gave rise to a narrow heat flow profile (Figure 3D), similar to the ones observed for 11(12)- and 14(15)EET, with a k_{cat} of 9.65 ± 0.19 sec^{-1} and a K_M of 2.98 ± 0.56 μM. As observed with the other substrates, negligible heat and product inhibition effects were observed in blank test injections (Figure S2B and S4).

Characterisation of hsEH CTD inhibition using ITC

We adapted a protocol that builds on SIM ITC enzyme kinetic measurements[21] to set up a versatile and continuous method to measure the inhibitory potency of hsEH antagonists against natural substrates, as well as readily characterise their mode of inhibition. We

7

evaluated the thermal power of 14(15)EET hydrolysis in the presence of the well-known hsEH inhibitor AUDA. The enzyme was placed in the calorimeter cell, whilst the syringe was loaded with a mixture of substrate and inhibitor. A series of injections was then performed (Figure 4A). In the experiment, AUDA accumulated in the sample cell with its concentration increasing 1-fold with each successive injection. This results in each injection producing a heat flow response that was progressively lower and broader than the preceding one, owing to increased hsEH CTD inhibition. Blank test injections showed little heat effects of substrate/inhibitor dilution into buffer (Figure S5A). Each peak injection was analysed individually to measure the ΔH_{app} and extract the Michaelis−Menten parameters. The k_{cat} values derived from each peak were identical (8.89 ± 1.64 sec^{-1}) and in agreement with the value detected in the absence of inhibitor (Table 1). The apparent K_M (K_M') for 14(15)EET increased at every successive injection with growing inhibitor concentration (Figure 4B). The k_{cat} and K_M' values obtained by this analysis indicate a model of competitive inhibition,[32] which is consistent with AUDA's reported mode of action.[26,33] As AUDA is a competitive inhibitor, the *y*-intercept of the K_M' *vs.* AUDA concentration plot (Figure 4B) provides the true K_M,[32] measured as 11.91 ± 3.43 μM, in concurrence with the value for the 14(15)EET substrate obtained in the absence of inhibitor (Table 1). The analysis of the slope of the straight line fitted to the data points gives the K_M'/K_i ratio,[32] providing an average K_i for AUDA of 7.62 ± 2.81 nM. This is in excellent agreement with the value obtained from a spectrofluorimetric assay using the synthetic substrate PHOME[28,29,34] (Figure S6A and B).

Discussion

The study of EpFA catalysis mediated by hsEH is severely limited by the unavailability of fast, simple and effective methods to study their kinetics of hydrolysis. The only technique available thus far is a LC-MS/MS-based methodology,[10] which, although highly sensitive, is a post-reaction ancillary technique, involving multiple steps of sample manipulation and analysis,[32] and requiring highly specialised equipment and technical expertise. To develop a truly general, versatile and rapid enzyme kinetics assay, we have developed a single-injection ITC (SIM) approach. By detecting the heat released or absorbed in real time during catalysis, this technique follows reactions of native substrates without the need of detectable changes in physicochemical properties to track the concentration of substrate or product over time. The single-injection ITC method yields both thermodynamic and kinetic parameters in a single experiment. Recent advances in instrumentation faster response times and analysis software

8

(*e.g.* the new PEAQ-ITC analysis software) have allowed this approach to become more user-friendly and routine. Compared to the multi-injection ITC method counterpart, the SIM is significantly faster, requires less enzyme, and is less subject to errors linked to baseline drift, or other time-dependent effects, including enzyme aggregation and/or precipitation and substrate degradation,[19] because of the reduced experimental time and faster data acquisition.[19,35]

The ITC single-injection application presented here enables the rapid characterisation of kinetic parameters of various natural EpFA substrates of hsEH, such as EETs, EpETEs, EpDPEs and EpOMEs, using small amounts of protein and substrate, with each experiment taking on average 50 minutes (including washing and preparation of the instrument). To our knowledge this is the first example of the ITC SIM applied to lipid catalysis and it is the only method to date that allows a quantitative analysis of hsEH-mediated hydrolysis of EpFAs in a continuous manner.

Our investigations revealed that all EpFAs tested could be hydrolysed by hsEH, albeit significant differences were observed in their kinetics profiles, in agreement with a previous study[10]. It is noteworthy that although data fitted well to the Michaelis-Menten model, hsEH CTD performs a two-step catalysis, undergoing first the formation of a covalent enzyme-substrate alkyl intermediate followed by its hydrolysis.[4,36] In these cases, K_M values describe the concentration of the substrate for which the catalytic rate is half maximal, instead of providing an accurate measure of the substrate affinity for the enzyme,[37] and k_{cat} values represent mainly the hydrolysis rate of the covalent intermediate, given that this second step of the hsEH CTD-mediated catalysis is at least an order of magnitude slower than the first (formation of the alkyl covalent intermediate).[4,36]

Our results (Table 1) indicate that K_M and k_{cat} values vary significantly depending on the chemical scaffold and the epoxide position on the fatty acid structure. Whereas variations of K_M values could not easily be correlated with substrate properties in this study, in general k_{cat} values were the largest when the epoxide was central, on the carbon positions 11, 12 and 14 of the fatty acid chain. Comparison of catalytic efficiency (K_{sp}), a measurement of the overall rate of the reaction and specificity of an enzyme for a substrate,[37] revealed the preferred EpFA targets for hsEH CTD, summarised in a heatmap (Figure 5). For the substrates tested in our study, the rank order of hsEH CTD catalytic preference is 12(13)EpOME > 11(12)EET > 14(15)EET > 8(9)EpETE > 19(20)EpDPE ≈ 8(9)EET > 17(18)EpETE > 5(6)EET. A trend is revealed here, correlating catalytic efficiency with the position of the epoxide function: hsEH

CTD distinctly prefers epoxides located in the middle of the fatty acid chain, at positions 11, 12 and 14, with its activity steadily decreasing for substrates bearing the epoxide moiety closer to either the carboxyl acid group or to the methyl group at the end of the hydrocarbon chain. Having the epoxide close the carboxyl function is the least preferred configuration, as indicated by the lowest efficiency for 5(6)EET. This appears consistent with the narrow 'L-shaped' hsEH CTD active site, with the catalytic triad positioned deep in the vertex and surrounded by two large hydrophobic regions.[1,6] Notably, the overall substrate preference for sEH revealed by ITC is largely in agreement with what was previously observed in Morisseau *et al.*[10] by LC-MS/MS, although it is noteworthy that the discrete Michaelis-Menten parameters do differ in the two studies (especially $k_{cat,}$).

Given that hsEH inhibition is a potential therapeutic approach in a number of pathological conditions, the detailed knowledge of hsEH catalytic efficiency towards its various substrates is of great importance, as it will inform on how such an inhibition will affect the metabolism of several EpFAs, enabling the prediction of the expected outcome from their altered levels. As the relative abundance of each epoxy-fatty acid varies within the organism,[10,13] a pharmacological intervention may have simultaneous assorted responses in different tissues and organs.

In addition to measuring the kinetics of catalysis for different EpFA targets of hsEH, we also devised an ITC method to screen new hsEH inhibitors using natural substrates. Our ITC application brings significant advantages. First, it evaluates inhibitor potency using hsEH physiological substrates, circumventing the problems associated with employing non-native fluorogenic compounds. This will have a particular bearing for the analysis of non-competitive and mixed inhibitors, which bind respectively to the enzyme-substrate complex or both to enzyme and substrate.[32] Interestingly, new allosteric inhibitors of hsEH have started to emerge,[34] increasing the timely relevance of this new methodology. Furthermore, as the efficacy of non-competitive and mixed inhibitors may in principle differ from substrate to substrate, our ITC method offers a well-suited solution for a systematic characterisation of inhibition versus a battery of EpFA substrates. As a second major benefit, the ITC method allows for a straightforward characterisation of the mode of inhibition (*i.e.* competitive, uncompetitive or non-competitive/mixed),[32] which is critical to drug development as evaluating the inhibitory power, given that it reveals the nature of the inhibited state(s).

1
2
3
4
5
6
7
8
9
10
11
12
13
14
15
16
17
18
19
20
21
22
23
24
25
26
27
28
29
30
31
32
33
34
35
36
37
38
39
40
41
42
43
44
45
46
47
48
49
50
51
52
53
54
55
56
57
58
59
60

Conclusions

Despite the crucial biological roles of hsEH in a variety of physiological and pathological states, a comprehensive understanding of its catalytic activity against a compendium of natural substrates remains inadequate. Equally, the availability of assays that characterise and screen hsEH inhibitors using native substrates has been limited to date. We have presented a novel, versatile, expedient and reliable ITC SIM application that has the potential to be adopted as method of choice to perform such characterisations. Being not reliant on specific physicochemical and spectroscopic properties, our method is ideally posed to facilitate the discovery of new putative epoxy substrates of hsEH. Moreover, calorimetric measurements can be performed in mixtures and suspensions, *e.g.* in cellular and crude tissue extracts, as well as allowing measurements over a range of biologically relevant conditions[19,38] (pH, redox conditions, salt concentration etc.), thereby having the potential to contribute to advances of hsEH biology in health and disease. As recent discoveries suggest a role for hsEH in redox regulatory systems,[39,40,34] our newly developed ITC method can be used to assess the impact of enzyme oxidative state on both catalysis and inhibition of EpFAs hydrolysis.

Taken together, our results show the first proof-of-concept for kinetic characterisation and inhibitor screening of hsEH activities using ITC, an approach which is generally applicable to other enzymes involved in lipid metabolism and should help in the search for novel inhibitors of this important class of enzymes.

11

Associated content

Supporting Information is available. It comprises 7 Figures and one Table reporting a schematic of the EpFAs metabolism, all the experimental controls and the spectrofluorimetric analysis of hsEH CTD inhibition. It also includes full experimental procedures and protocols, as well as a full mathematical treatment of the theoretical basis of kinetic rates determination by ITC.

Authors information

Corresponding author: Maria R Conte: 0000-0001-8558-2051

Tam TT Bui: 0000-0002-8074-4928

Giancarlo Abis: 0000-0003-1440-7832

Raúl Pacheco-Gómez: 0000-0001-6932-9734

Author's contribution

MRC, GA and RPG contributed to the planning and the design of the study. GA prepared the recombinant enzyme used in all the experiments and performed the spectrofluorometric analysis. GA, RPG and MRC optimised the experimental set up for the ITC kinetics analysis. GA and TTTB performed the ITC experiments for both kinetics and inhibition studies. MRC, GA and RPG participated to the data analysis and contributed to the writing of the manuscript. MRC obtained funding for this work.

Notes

The authors declare no competing financial interest.

Acknowledgements

Tables

Substrate	ΔH_{app} [kJ mol^{-1}]	k_{cat} [sec^{-1}]	K_M [µM]	K_{sp} [sec^{-1} µM^{-1}]
5(6)EET	-4.84 ± 0.65	0.35 ± 0.05	46.61 ± 10.98	0.01± 0.001
8(9)EET	-39.45 ± 3.88	1.28 ± 0.19	23.10 ± 2.39	0.054 ± 0.010
11(12)EET	-12.43 ± 0.62	4.31 ± 0.16	1.74 ± 0.20	2.53 ± 0.25
14(15)EET	-23.72 ± 3.46	6.64 ± 1.54	12.88 ± 1.94	0.527 ± 0.075
8(9)EpETE	-34.13 ± 0.93	1.61 ± 0.01	9.74 ± 0.13	0.173 ± 0.006
17(18)EpETE	-51.78 ± 1.73	0.64 ± 0.06	26.37 ± 4.05	0.025 ± 0.003
19(20)EpDPE	-23.73 ± 1.82	1.62 ± 0.08	26.60 ± 1.21	0.061 ± 0.003
12(13)EpOME	-5.67 ± 0.38	9.65 ± 0.19	2.98 ± 0.56	3.56 ± 0.86

Table 1. Mean and standard error values for the apparent enthalpy and kinetics parameters of hsEH CTD-mediated hydrolysis of the EpFAs analysed in this study. The values were obtained as described in the methods.

Figure Legends

Figure 1. Quantitative characterisation of hsEH-mediated hydrolysis of 14(15)EET. (A) Representative thermal profile of a single-injection of 14(15)EET into hsEH CTD. (B) Screenshot from the MicroCal PEAQ-ITC Analysis Software. The ΔH_{app} was calculated by integrating the area under the peak (violet), upon definition of the baseline through manual adjustments of the left markers workspace (green). The data points used for the Michaelis–Menten kinetics curve fitting were obtained by manual adjustments of the right markers workspace (grey), selecting the window between the end of the injection (maximum substrate concentration – saturating enzyme conditions) and the end of the decaying portion of the peak (minimum substrate concentration – beginning of the kinetics curve). Note that the first part of the curve corresponding to substrate injection was not included in the rate plot analysis. (C) Representative Michaelis–Menten fit of the $\{[S]_i; v_i\}$ data point extrapolated from B using the MicroCal PEAQ-ITC Analysis Software analysis.

Figure 2. Single-injection isotherms and data fitting for the hsEH-mediated hydrolysis of EETs. Experiments are shown for (A) 5(6)EET; (B) 8(9)EET and (C) 11(12)EET. Each panel reports a representative thermal profile of a single-injection experiment (top plot) and the corresponding data fit using the Michaelis–Menten model (bottom plot). Note that the faster the reaction, the fewer data points will be available for fitting the plot.

Figure 3. Single-injection isotherms and data fitting for the hsEH-mediated hydrolysis of EpFAs. Experiments are shown for (A) 8(9)EpETE; (B) 17(18)EpETE; (C) 19(20)EpDPE and (D) 12(13)EpOME. Each panel reports a representative thermal profile of a single-injection experiment (top plot) and the corresponding data fit using the Michaelis–Menten model (bottom plot). Note that for faster reactions fewer data points will be available for fitting the plot.

Figure 4. hsEH CTD inhibition studies. (A) Representative thermal power of 14(15)EET/AUDA injections into hsEH CTD. The magnitude of the peaks decreases with each successive injection due to the increased concentration of the inhibitor, whilst the slope of the recovery increased, suggesting a competitive mode of inhibition. (B) Linear K_M' *vs.* AUDA concentration fitting from data shown in (A).

Figure 5. Heatmap of the kinetics parameters of the hsEH CTD-mediated hydrolysis of EpFAs showing K_{sp}. inverse of K_M (K_M^{-1} [μM^{-1}]) and k_{cat}. Colours span from grey to dark red

with increasing values. Each shade of grey-to-red indicates an increase of the 12.5th percentile of the total interval of values. A combination of dark red shades indicates high affinity, turnover rate, and efficiency.

15

References

(1)   Argiriadi, M. a; Morisseau, C.; Hammock, B. D.; Christianson, D. W. Detoxification of environmental mutagens and carcinogens: structure, mechanism, and evolution of liver epoxide hydrolase. *Proc. Natl. Acad. Sci. U. S. A.* **1999**, *96*, 10637–10642. https://doi.org/10.1073/pnas.96.19.10637.

(2)   Gomez, G. A.; Morisseau, C.; Hammock, B. D.; Christianson, D. W. Structure of human Epoxide Hydrolase reveals mechanistic inferences on bifunctional catalysis in epoxide and phosphate ester hydrolysis. **2004**, *43*, 4716–4723. https://doi.org/10.1021/bi036189j.

(3)   Borhan, B.; Jones, D. A.; Pinot, F.; Grant, D. F.; Kurth, M. J.; Hammock, B. D. Mechanism of Soluble Epoxide Hydrolase. *J. Biol. Chem.* **1995**, *270* (45), 26923–26930.

(4)   Morisseau, C.; Hammock, B. D. Epoxide Hydrolases: mechanisms, inhibitor designs, and biological roles. *Annu. Rev. Pharmacol. Toxicol.* **2005**, *45* (1), 311–333. https://doi.org/10.1146/annurev.pharmtox.45.120403.095920.

(5)   Argiriadi, M. A.; Morisseau, C.; Goodrow, M. H.; Dowdy, D. L.; Hammock, B. D.; Christianson, D. W. Binding of alkylurea inhibitors to epoxide hydrolase implicates active site tyrosines in substrate activation. *J. Biol. Chem.* **2000**, *275* (20), 15265–15270. https://doi.org/10.1074/jbc.M000278200.

(6)   Gomez, G. A.; Morisseau, C.; Hammock, B. D.; Christianson, D. W. Human soluble epoxide hydrolase : Structural basis of inhibition by 4-(3-cyclohexylureido)-carboxylic acids. *Protein Sci.* **2006**, *15*, 58–64. https://doi.org/10.1110/ps.051720206.58.

(7)   Imig, J. D. Epoxides and soluble Epoxide Hydrolase in cardiovascular physiology. *Physiol. Rev.* **2012**, *92* (1), 101–130. https://doi.org/10.1152/physrev.00021.2011.

(8)   Spector, A. A.; Fang, X.; Snyder, G. D.; Weintraub, N. L. Epoxyeicosatrienoic acids (EETs): Metabolism and biochemical function. *Prog. Lipid Res.* **2004**, *43* (1), 55–90. https://doi.org/10.1016/S0163-7827(03)00049-3.

(9)   Capdevila, J. H.; Falck, J. R.; Harris, R. C. Cytochrome P450 and arachidonic acid bioactivation. Molecular and functional properties of the arachidonate monooxygenase. *J. Lipid Res.* **2000**, *41*, 163–181.

(10)   Morisseau, C.; Inceoglu, B.; Schmelzer, K.; Tsai, H.-J.; Jinks, S. L.; Hegedus, C. M.; Hammock, B. D. Naturally occurring monoepoxides of eicosapentaenoic acid and docosahexaenoic acid are bioactive antihyperalgesic lipids. *J. Lipid Res.* **2010**, *51* (12), 3481–3490. https://doi.org/10.1194/jlr.M006007.

(11)   Gabbs, M.; Leng, S.; Devassy, J. G.; Monirujjaman, M.; Aukema, H. M. Advances in Our Understanding of Oxylipins Derived from Dietary PUFAs. *Adv. Nutr.* **2015**, *6* (5), 513–540. https://doi.org/10.3945/an.114.007732.

(12)   Mitchell, L. A.; Grant, D. F.; Melchert, R. B.; Petty, N. M.; Kennedy, R. H. Linoleic acid metabolites act to increase contractility in isolated rat heart. *Cardiovasc. Toxicol.* **2002**, *2* (3), 219–229. https://doi.org/10.1385/CT:2:3:219.

(13)   Gabbs, M.; Leng, S.; Devassy, J. G.; Monirujjaman, M.; Aukema, H. M. Advances in

16

Our Understanding of Oxylipins Derived from Dietary PUFAs. *Adv. Nutr.* **2015**, *6* (5), 513–540. https://doi.org/10.3945/an.114.007732.

(14) Zhang, G.; Panigrahy, D.; Mahakian, L. M.; Yang, J.; Liu, J.-Y.; Lee, K. S. S.; Wettersten, H. I.; Ulu, A.; Hu, X.; Tam, S; Hwang S. H.; Ingham E. S.; Kieran M. W.; Weiss R. H.; Ferrara K. W.; Hammock B. D. Epoxy metabolites of docosahexaenoic acid (DHA) inhibit angiogenesis, tumor growth, and metastasis. *Proc. Natl. Acad. Sci. U. S. A.* **2013**, *110* (16), 6530–6535. https://doi.org/10.1073/pnas.1304321110/-/DCSupplemental.www.pnas.org/cgi/doi/10.1073/pnas.1304321110.

(15) Ulu, A.; Harris, T. R.; Morisseau, C.; Miyabe, C.; Inoue, H.; Schuster, G.; Dong, H.; Iosif, A.-M.; Liu, J.-Y.; Weiss, R. H.; Chiamvimonvat N.; Imig J. D.; Hammock B. D. Anti-inflammatory effects of ω-3 polyunsaturated fatty acids and soluble epoxide hydrolase inhibitors in angiotensin-II-dependent hypertension. *J. Cardiovasc. Pharmacol.* **2013**, *62* (3), 285–297. https://doi.org/10.1097/FJC.0b013e318298e460.

(16) Hu, J.; Dziumbla, S.; Lin, J.; Bibli, S.; Zukunft, S.; de Mos, J.; Awwad, K.; Frömel, T.; Jungmann, A.; Devraj, K.; Cheng Z.; Wang L.; Fauser S.; Eberhart C. G.; Sodhi A.; Hammock B. D.; Liebner S.; Müller O. J.; Glaubitz C.; Hammes H. P.; Popp R.; Fleming I. Inhibition of soluble epoxide hydrolase prevents diabetic retinopathy. *Nature* **2017**, *552*, 248–252. https://doi.org/10.1038/nature25013.

(17) Moran, J. H.; Weise, R.; Schnellmann, R. G.; Freeman, J. P.; Grant, D. F. Cytotoxicity of linoleic acid diols to renal proximal tubular cells. *Toxicol. Appl. Pharmacol.* **1997**, *146* (1), 53–59. https://doi.org/10.1006/taap.1997.8197.

(18) El-Sherbeni, A. A.; El-Kadi, A. O. S. The role of epoxide hydrolases in health and disease. *Arch. Toxicol.* **2014**, *88* (11), 2013–2032. https://doi.org/10.1007/s00204-014-1371-y.

(19) Mazzei, L.; Ciurli, S.; Zambelli, B. *Isothermal Titration Calorimetry to Characterize Enzymatic Reactions*, 1; Elsevier Inc., 2016; ج.م. 567. https://doi.org/10.1016/bs.mie.2015.07.022.

(20) Di Trani, J. M.; Moitessier, N.; Mittermaier, A. K. Measuring Rapid Time-Scale Reaction Kinetics Using Isothermal Titration Calorimetry. *Anal. Chem.* **2017**, *89* (13), 7022–7030. https://doi.org/10.1021/acs.analchem.7b00693.

(21) Di Trani, J. M.; Moitessier, N.; Mittermaier, A. K. Complete Kinetic Characterization of Enzyme Inhibition in a Single Isothermal Titration Calorimetric Experiment. *Anal. Chem.* **2018**, *90* (14), 8430–8435. https://doi.org/10.1021/acs.analchem.8b00993.

(22) Todd, M. J.; Gomez, J. Enzyme kinetics determined using calorimetry: a general assay for enzyme activity? *Anal. Biochem.* **2001**, *296* (2), 179–187. https://doi.org/10.1006/abio.2001.5218.

(23) Transtrum, M. K.; Hansen, L. D.; Quinn, C. Enzyme kinetics determined by single-injection isothermal titration calorimetry. *Methods* **2015**, *76*, 194–200. https://doi.org/10.1016/j.ymeth.2014.12.003.

(24) Wagner, K. M.; McReynolds, C. B.; Schmidt, W. K.; Hammock, B. D. Soluble epoxide hydrolase as a therapeutic target for pain, inflammatory and neurodegenerative diseases. *Pharmacol. Ther.* **2017**, *180*, 62–76. https://doi.org/10.1016/j.pharmthera.2017.06.006.

17

(25)   Imig, J.; Hammock, B. Soluble epoxide hydrolase as a therapeutic target for cardiovascular diseases. *Nat. Rev. Drug Discov.* **2009**, *8* (10), 794–805. https://doi.org/10.1038/nrd2875.Soluble.

(26)   Shen, H. C.; Hammock, B. D. Discovery of inhibitors of soluble Epoxide Hydrolase: A target with multiple potential therapeutic indications. *J. Med. Chem.* **2012**, *55* (5), 1789–1808. https://doi.org/10.1021/jm201468j.

(27)   Morisseau, C.; Hammock, B. D. Measurement of soluble epoxide hydrolase (sEH) activity. *Curr. Protoc. Toxicol.* **2007**, *Chapter 4*, 4.23.1-4.23.18. https://doi.org/10.1002/0471140856.tx0423s33.

(28)   Wolf, N. M.; Morisseau, C.; Jones, P. D.; Hock, B.; Hammock, B. D. Development of a high-throughput screen for soluble epoxide hydrolase inhibition. *Anal. Biochem.* **2006**, *355*, 71–80. https://doi.org/10.1016/j.ab.2006.04.045.

(29)   Abis, G.; Charles, R. L.; Eaton, P.; Conte, M. R. Expression, purification, and characterisation of human soluble Epoxide Hydrolase (hsEH) and of its functional C-terminal domain. *Protein Expr. Purif.* **2019**, *153* (July 2018), 105–113. https://doi.org/10.1016/j.pep.2018.09.001.

(30)   Hansen, L. D.; Transtrum, M. K.; Quinn, C.; Demarse, N. Enzyme-catalyzed and binding reaction kinetics determined by titration calorimetry. *Biochim. Biophys. Acta - Gen. Subj.* **2016**, *1860* (5), 957–966. https://doi.org/10.1016/j.bbagen.2015.12.018.

(31)   Luo, Q.; Chen, D.; Boom, R. M.; Janssen, A. E. M. Revisiting the enzymatic kinetics of pepsin using isothermal titration calorimetry. *Food Chem.* **2018**, *268* (June), 94–100. https://doi.org/10.1016/j.foodchem.2018.06.042.

(32)   Copeland, R. A. *Evaluation of enzyme inhibitors in drug discovery*, First.; Wiley, 2005.

(33)   Kim, I.; Morisseau, C.; Watanabe, T.; Hammock, B. D. Design, synthesis, and biological activity of 1,3-disubstituted ureas as potent inhibitors of the soluble epoxide hydrolase of increased water solubility Solubility. *J. Med. Chem.* **2004**, *47* (8), 2110–2122.

(34)   Abis, G.; Charles, R. L.; Kopec, J.; W Yue, W.; Atkinson, R. A.; Bui, T. T.; Lynham, S.; Popova, S.; Sun, Y.-B.; Fraternali, F.; Eaton P.; Maria R. C. 15-deoxy-Δ12,14-Prostaglandin J2-mediated inhibition reveals two allosteric sites of the human soluble Epoxide Hydrolase. *Commun. Biol.*

(35)   Hansen, L. D.; Transtrum, M. K.; Quinn, C.; Demarse, N. Enzyme-catalyzed and binding reaction kinetics determined by titration calorimetry. *Biochim. Biophys. Acta - Gen. Subj.* **2016**, *1860* (5), 957–966. https://doi.org/10.1016/j.bbagen.2015.12.018.

(36)   Hopmann, K. H.; Himo, F. Insights into the reaction mechanism of soluble epoxide hydrolase from theoretical active site mutants. *J. Phys. Chem. B* **2006**, *110* (42), 21299–21310. https://doi.org/10.1021/jp063830t.

(37)   Price, N. C.; Lewis, S. *Fundamentals of enzymology*, Third.; Press, O. U., محرر; 1999.

(38)   Freyer, M. W.; Edwin, L. A. Isothermal Titration Calorimetry: Experimental Design, Data Analysis, and Probing Macromolecule/Ligand Binding and Kinetic Interactions. *Methods Cell Biol.* **2008**, *84*, 79–113. https://doi.org/doi.org/10.1016/S0091-679X(07)84004-0.

18

(39)   Charles, R. L.; Burgoyne, J. R.; Mayr, M.; Weldon, S. M.; Hubner, N.; Dong, H.; Morisseau, C.; Hammock, B. D.; Landar, A.; Eaton, P. Redox regulation of soluble epoxide hydrolase by 15-Deoxy-delta-Prostaglandin J2 controls coronary hypoxic vasodilation. *Circ. Res.* **2011**, *108* (3), 324–334. https://doi.org/10.1161/CIRCRESAHA.110.235879.

(40)   Charles, R. L.; Rudyk, O.; Prysyazhna, O.; Kamynina, A.; Yang, J.; Morisseau, C.; Hammock, B. D.; Freeman, B. a; Eaton, P. Protection from hypertension in mice by the Mediterranean diet is mediated by nitro fatty acid inhibition of soluble epoxide hydrolase. *Proc. Natl. Acad. Sci. U. S. A.* **2014**, *111* (22), 8167–8172. https://doi.org/10.1073/pnas.1402965111.

1
2
3
4
5
6
7
8
9
10
11
12
13
14
15
16
17
18
19
20
21
22
23
24
25
26
27
28
29
30
31
32
33
34
35
36
37
38
39
40
41
42
43
44
45
46
47
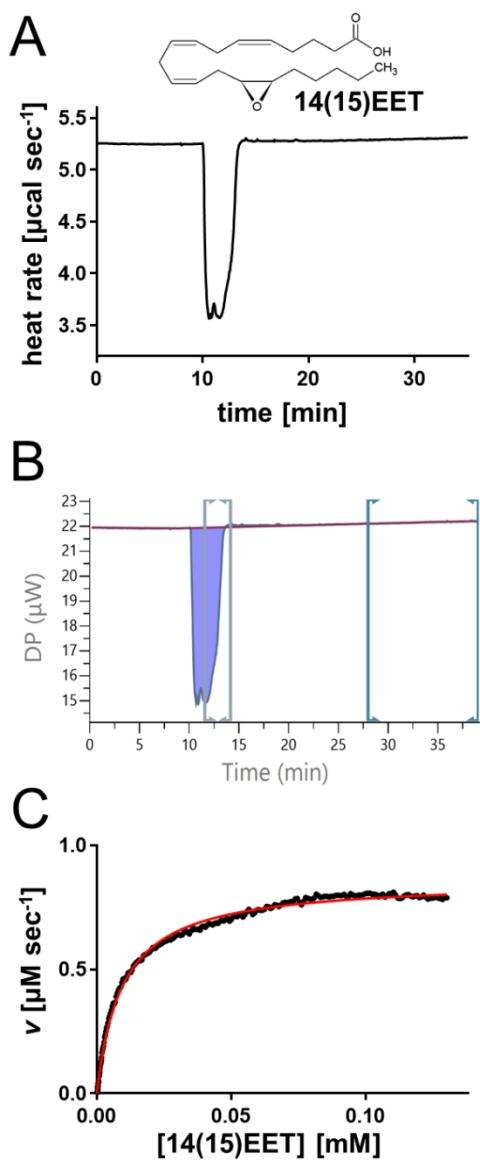48
49
50
51
52
53
54
55
56
57
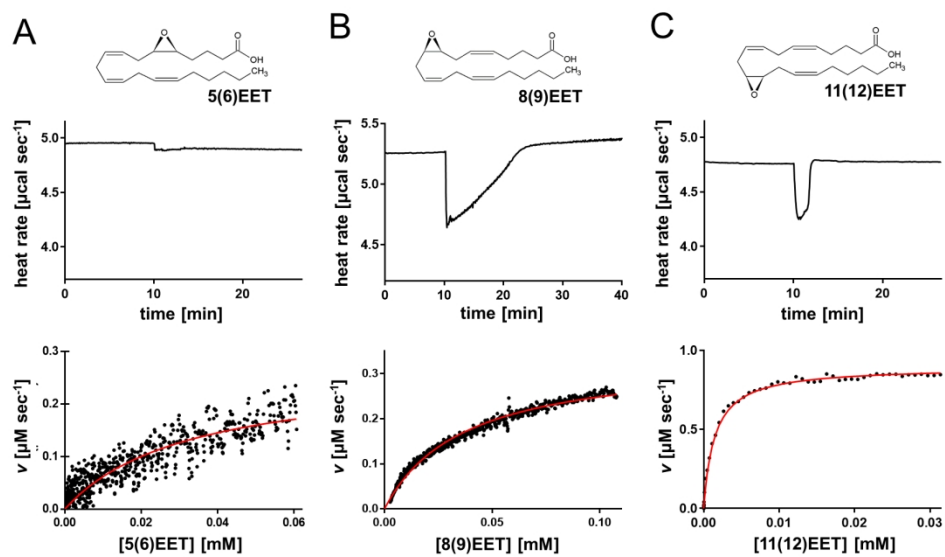58
59
60

Figure 1

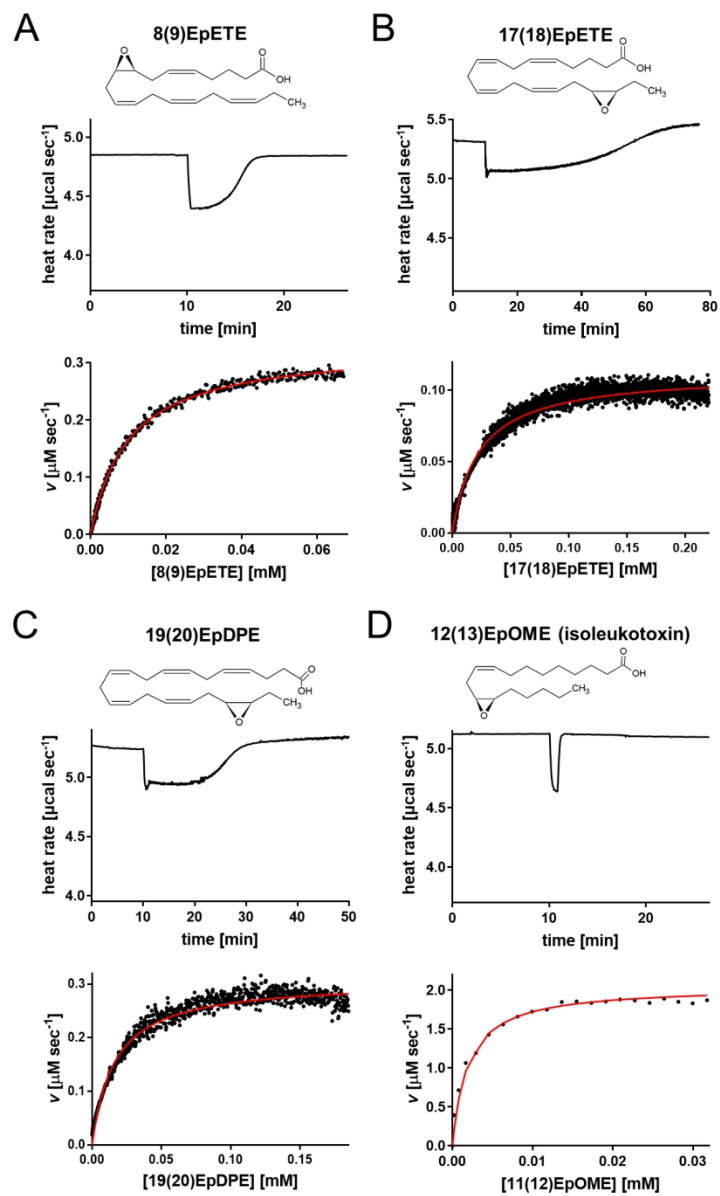55x122mm (300 x 300 DPI)

Figure 2

160x97mm (300 x 300 DPI)

Figure 3

110x177mm (300 x 300 DPI)

1
2
3
4
5
6
7
8
9
10
11
12
13
14
15
16
17
18
19
20
21
22
23
24
25
26
27
28
29
30
31
32
33
34
35
36
37
38
39
40
41
42
43
44
45
46
47
48
49
50
51
52
53
54
55
56
57
58
59
60
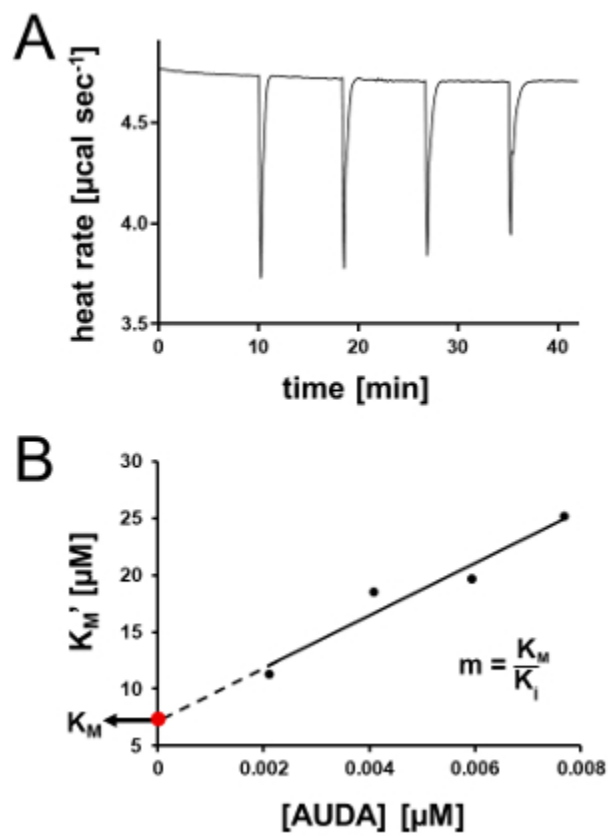
Figure 4

26x37mm (300 x 300 DPI)
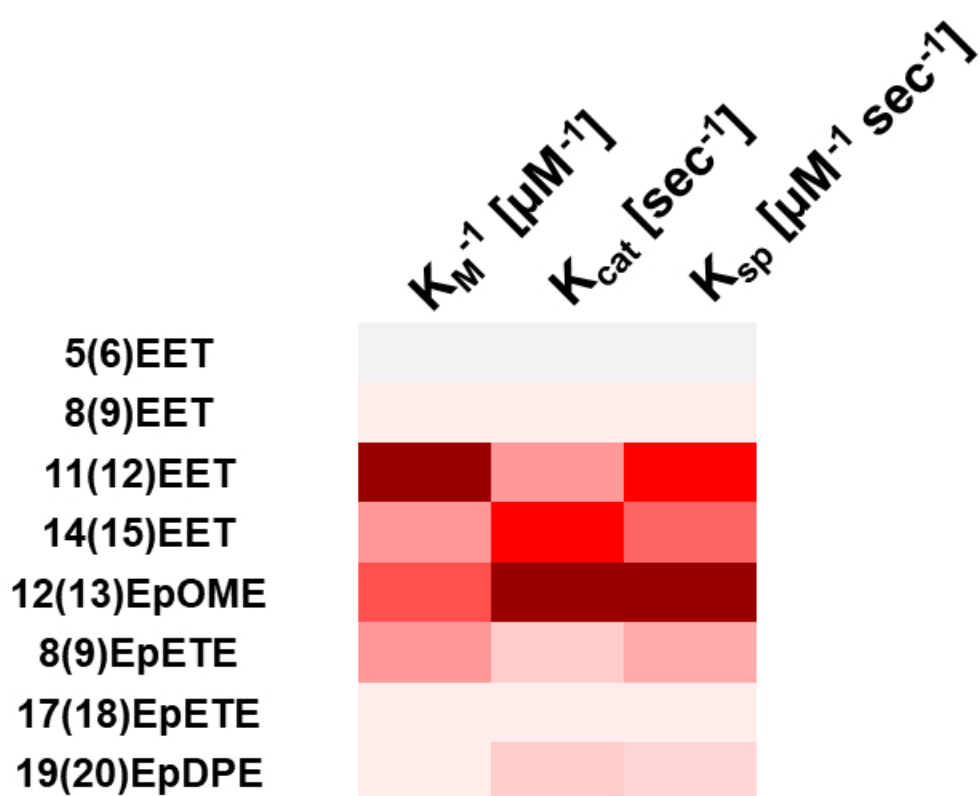
Figure 5

52x44mm (300 x 300 DPI)

1
2
3
4
5
6
7
8
9
10
11
12
13
14
15
16
17
18
19
20
21
22
23
24
25
26
27
28
29
30
31
32
33
34
35
36
37
38
39
40
41
42
43
44
45
46
47
48
49
50
51
52
53
54
55
56
57
58
59
60
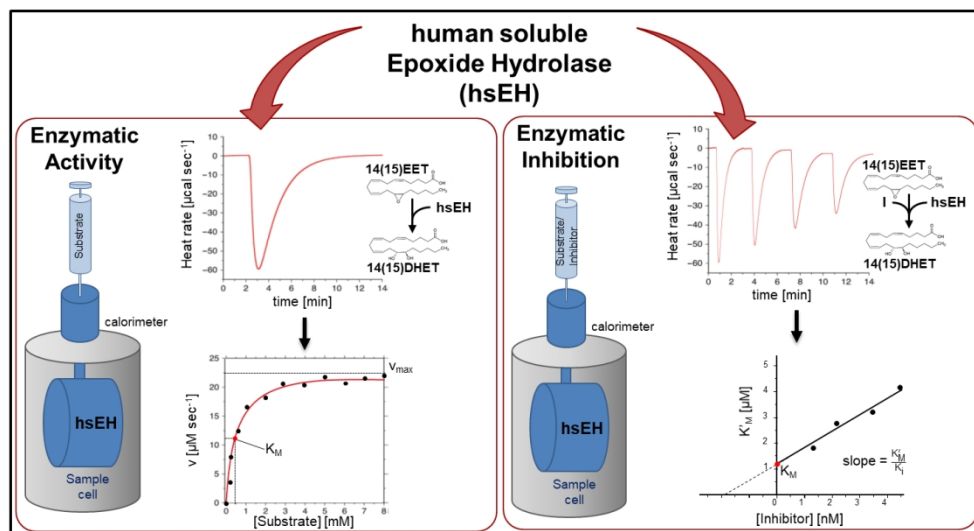
Graphical abstract

127x67mm (300 x 300 DPI)